Applied Mathematical Modelling 36 (2012) 3153–3160

Contents lists available at SciVerse ScienceDirect

Applied Mathematical Modelling

journal homepage: www.elsevier.com/locate/apm

Extracting energy from Vortex-Induced Vibrations: A parametric study

Antonio Barrero-Gil [a,*], Santiago Pindado [b], Sergio Avila [b]

[a] Aerospace Propulsion and Fluid Mechanics Department, School of Aeronautics, Universidad Politecnica de Madrid, Plaza Cardenal Cisneros 3, E-28040 Madrid, Spain

[b] Instituto Universitario 'Ignacio Da Riva', Universidad Politecnica de Madrid, Plaza Cardenal Cisneros 3, E-28040 Madrid, Spain

ARTICLE INFO

Article history:
Received 29 April 2011
Received in revised form 21 September 2011
Accepted 29 September 2011
Available online 12 October 2011

Keywords:
Vortex-Induced-Vibration
Energy harvesting
Efficiency

ABSTRACT

Here, Vortex-Induced Vibrations (VIVs) of a circular cylinder are analyzed as a potential source for energy harvesting. To this end, VIV is described by a one-degree-of-freedom model where fluid forces are introduced from experimental data from forced vibration tests. The influence of some influencing parameters, like the mass ratio m^* or the mechanical damping ζ in the energy conversion factor is investigated. The analysis reveals that: (i) the maximum efficiency η_M is principally influenced by the mass-damping parameter $m^*\zeta$ and there is an optimum value of $m^*\zeta$ where η_M presents a maximum; (ii) the range of reduced velocities with significant efficiency is mainly governed by m^*, and (iii) it seems that encouraging high efficiency values can be achieved for high Reynolds numbers.

1. Introduction

When an elastic bluff body is under the action of a steady fluid flow, for high enough Reynolds numbers (Re > 100, say) the flow separates from the body surface generating an unsteady broad wake. Typically, the flow pattern is characterized by two shear layers on each side of the body that are unstable and roll up to form vortices [1]. These vortices are shed to the wake periodically with a frequency f_T that is related to the undisturbed flow speed U and the size of the cross-section body D by the well known Strouhal relationship, $St = f_T D/U$ (being St the Strouhal number). As the flow velocity is increased from zero, the vortex shedding frequency increases and there is a flow velocity at which vortex shedding has a frequency close to the body's natural frequency of oscillations f_N and, for low values of the mass and mechanical properties, significant oscillations can be induced in the body. When the body is oscillating a complex interaction between the oscillating body and flow field around it develops, where two features must be outlined: (i) there is a range of flow velocities where vortex shedding frequency is synchronized with the frequency of oscillation (*lock-in* regime), giving for significant oscillations and (ii) the cylinder response may exhibit hysteresis, with jumps in oscillation amplitude and in the fluid forces acting on the body. This non-linear resonance phenomenon is known as Vortex-Induced Vibration (VIV) and it has much relevance in several branches of mechanical engineering. For example, it can be observed in civil structures, like slender chimneys stacks, tall buildings, electric power lines or bridges, to name a few. It is also usual in offshore structures or in the tubes of heat exchange devices. Because its practical and scientific interest, VIV has lead to a large number of fundamental studies, many of which are reviewed by Bearman [2], Sarpkaya [3], and Williamson and Govardhan [4].

Usually, VIV is considered as an undesirable effect, as it may seriously affect the structural integrity or the reliability of performance, but along this paper we will show that if the vibration is substantial, it can be used to extract useful energy from the surrounding flow. This is not a new idea and Bernitsas et al. [5] have developed a very interesting device they called VIVACE (Vortex Induced Vibration Aquatic Clean Energy) that uses the oscillations induced by vortex shedding from a

* Corresponding author.
E-mail address: antonio.barrero@upm.es (A. Barrero-Gil).

0307-904X/$ - see front matter © 2011 Elsevier Inc. All rights reserved.
doi:10.1016/j.apm.2011.09.085

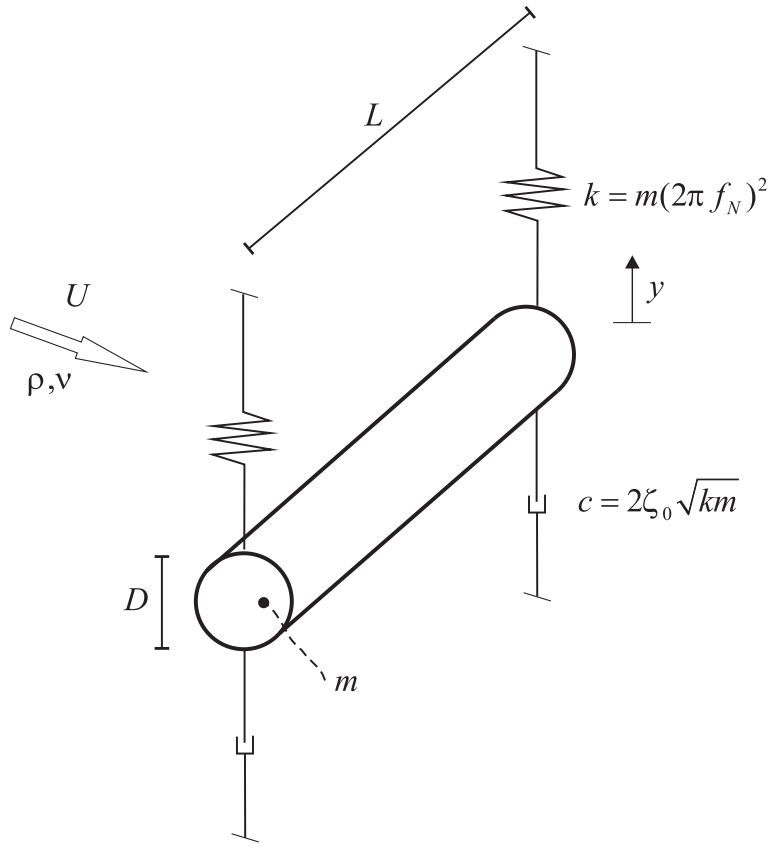

Fig. 1. Canonical VIV arrangement.

spring-mounted circular cylinder in a range of flow velocities to generate electricity. Other approaches to extract efficiently energy from a flow induced vibration phenomenon has been recently analyzed [6,7].

There are some relevant parameters controlling VIV of a spring-mounted circular cylinder (and hence the energy extraction), like the mass ratio m^* (i.e. the dimensionless number typifying the ratio of the mean density of the body to the density of the surrounding fluid), the mechanical damping ζ, the reduced velocity U^* (i.e. the relative importance of the convective acceleration to the local acceleration of the flow), the Reynolds number Re, or the aspect ratio L/D (see Fig. 1), and it would be very interesting to understand how the energy extraction (or efficiency) depends on these governing parameters. The main goal of this paper is to study in a systematic way the role of the mass and mechanical parameters (m^*, ζ) in the energy conversion for the simplified case of a spring-mounted circular cylinder, and try to give response to some unanswered questions that come to mind, such as *What is the maximum efficiency attainable as a function of the mechanical parameters*? or *Which is the range of reduced velocity where efficiency is significant*? or *How much is the Reynolds numbers influence*?

In an attempt to answer these questions, we have computed numerically the efficiency of energy conversion in the (m^*, ζ) space using experimental information from Hover et al. [8]. The influence of the Reynolds number is also investigated taking into account experimental results at a larger Reynolds number from Gopalkrishnan [9]. The results, presented appropriately later along the paper, seem to show that the mechanical-damping parameter (the product $m^*\zeta$) governs the maximum efficiency attainable, whereas the mass ratio is the main parameter controlling the range of reduced velocities where efficiency is significant.

We begin in Section 2 introducing a simple mathematical model of VIV, which helps to discuss some well established experimental facts, as well as to introduce an energy conversion factor. Based on this model, a parametric study is carried out in Section 3 revealing the role of the different parameters involved in the problem. Finally, some conclusions are drawn in Section 4.

2. Energy transfer and efficiency

2.1. Mathematical model of a circular cylinder undergoing VIV

For the sake of clarity, here we will consider the simplified case of a spring-mounted circular cylinder prone to oscillate in the transverse direction y under the action of an incoming flow (see sketch in Fig. 1). The system has a mass per unit length

m, and natural frequency of oscillations f_N. Let us also assume that the internal dissipation of the system can be described by a damping ratio $\zeta = c/(4\pi m f_N)$ where c is the mechanical damping constant. Then, the equation governing the transversal displacement of the cylinder is given by the interplay between the inertial, damping, stiffness, and fluid forces, namely,

$$m(\ddot{y} + 2\zeta\omega_N\dot{y} + \omega_N^2 y) = F_Y(t), \tag{1}$$

where the dot symbol stands for differentiation with respect to physical time t.

Experiments show that in the lock-in region (or resonance range), to a good approximation the fluid force per unit length can be described as

$$F_Y = \frac{1}{2}\rho U^2 D C_Y(t) = \frac{1}{2}\rho U^2 D C_Y \sin(2\pi f t + \phi), \tag{2}$$

where f is the oscillation frequency and ϕ is the phase angle by which the fluid force leads the cylinder displacement [2]. Substituting Eq. (2) in Eq. (1), considering (based on experimental evidences) a steady state of harmonic oscillations $y(t) = A\sin(2\pi f t)$, and equating sine and cosine terms, the solution for the normalized amplitude $A^* = A/D$ and normalized frequency $f^* = f/f_N$ is

$$A^* = \frac{C_Y \sin\phi}{16\pi^2 m^* \zeta}\left(\frac{U^{*2}}{f^*}\right), \tag{3a}$$

$$f^* = \left(1 - \frac{C_Y \cos\phi U^{*2}}{8\pi^2 m^* A^*}\right)^{1/2}. \tag{3b}$$

For large mass ratio, $m^* \gg 1$, from Eq. (3b) one can see that $f^* \simeq 1$ ($U^{*2}/8\pi \sim 1$ and experiments show that $C_Y\cos\phi \sim 1$). Then, one may deduce that, in this case, the response amplitude is just a function of the combined mass-damping parameter ($m^*\zeta$) and the reduced velocity U^*. For $m^* \sim 1$, however, Eqs. (3a) and (3b) are coupled and hence A^* should be a function of two independent parameters m^* and ζ, as well as U^*.

2.2. Efficiency

It is well known that the energy transfer can be quantified in terms of work done per unit length by the fluid over one cycle of oscillation T. Then, it is possible to introduce a conversion factor (or efficiency) η defined by the ratio of the mean power imparted by the flow to the body per unit length P_{F-B} and the total power in the flow per unit length P_F, that is

$$\eta = P_{F-B}/P_F, \tag{4}$$

where the total power in the flow per unit length is $\rho U^3 D/2$. The power extracted from the flow by the oscillating body, per cycle of oscillation T and per unit length, is given by

$$P_{F-B} = \frac{1}{T}\int_0^T F_y \dot{y}\, dt. \tag{5}$$

Considering a steady state of sinusoidal oscillations with amplitude A and frequency f it follows from Eqs. (2) and (4) that the conversion factor can be expressed in terms of the normalized amplitude, normalized velocity, normalized frequency, and the fluid force excitation coefficient $C_Y\sin\phi$,

$$\eta = \pi A^* C_Y \sin\phi\left(\frac{f^*}{U^*}\right). \tag{6}$$

From Eq. (6), we see that, for a particular Reynolds regime and fixed mechanical properties (m^* and ζ), computation of efficiency needs for the knowledge of the fluid force coefficients ($C_Y\sin\phi$ and $C_Y\cos\phi$) as a function of the normalized amplitude of oscillation and the true reduced velocity $V^* = U/(fD) = U^*/f^*$.

Finally, it should be noted that efficiency can also be defined considering the total area covered by the oscillating device during its motion. In that case, $\tilde{\eta} = P_{F-B}/P_{F*}$, where $P_{F*} = \rho U^3(2A + D)/2$, and it is easy to check that $\tilde{\eta} = \eta/(1 + 2A^*)$.

3. Results

For the numerical computation of the efficiency (Eq. (6)) as a function of the key parameters m^* and ζ (note that they can be chosen appropriately at the design stage) we have used experimental measured values of the fluid coefficients $C_Y\sin\phi$ and $C_Y\cos\phi$ in the parameter space (A^*, V^*). Observe that the influence of the Reynolds number is implicit in the fluid coefficients. To this end, Eqs. (3a) and (3b) have been solved iteratively. To this end, the following steps were given:

- Step 1. A value of the true reduced velocity V^* is fixed.
- Step 2. The normalized amplitude and normalized frequency are increased (A^* ranging from 0 to 1 in steps of 0.005 and f^* ranging from 0.5 to 1.5) until both Eqs. (3a) and (3b) are satisfied within a prescribed tolerance. At step i one can define two residuals, $res1_i = A_i^* - \frac{C_Y \sin\phi(A_i^*, V^*)}{16\pi^2 m^*\zeta}\left(\frac{U_i^{*2}}{f_i^*}\right)$ and $res2_i = f_i^* - \left(1 - \frac{C_Y\cos\phi(A_i^*, V^*)U_i^{*2}}{8\pi^2 m^* A_i^*}\right)^{1/2}$. Observe that $U_i^* = V^* f_i^*$. Values of $C_Y\sin\phi(A_i^*, V^*)$ and $C_Y\cos\phi(A_i^*, V^*)$ have been computed by 2D spline interpolation from the experimental database.

- Step 3. When both $|res1_i| < 0.01$ and $|res2_i| < 0.01$ the process is finished and $f_s^* = f_i^*,\ A_s^* = A_i^*,\ U_s^* = V^* f_i^*$.
- Step 4. The true reduced velocity is increased in a step of 0.1 and the procedure is repeated (the range of reduced velocities covered was 4–14).

Operating in this way, we can compute the efficiency (see Eq. (6)) in the A^*–U^* plane. Finally, we may note there is two identifiable sources of error for efficiency computation: (i) an error in the interpolated value selected for the fluid coefficients, and (ii) the error in the numerical evaluation of A^* from Eqs. (3a) and (3b). In the first case 2D spline numerical interpolation was used with a computed relative error less than 0.05. In the second case the dimensionless amplitude of oscillation is computed with an accuracy of 0.005, so that a relative error less than 0.1 can be estimated for $A^* > 0.05$ (only results with $A^* > 0.05$ are of interest). Taking into account these aspects we can estimate a relative error less than 0.15 for our computations.

3.1. Influence of the m^* regime

As already stated, efficiency can be computed if information is available on fluid coefficients from free or vibration controlled experiments. Here, the fluid coefficients measured by Hover et al. [8] by means of forced oscillations of a circular cylinders under the action of a stream of water ($Re = UD/\nu = 3800$, being ν the kinematic viscosity of the fluid, and $L/D = 19$) are used (see Fig. 2). In such forced vibration experiments, the cylinder were driven to be oscillating across the uniform flow (at certain free-stream velocity) with fixed amplitude and frequency. The fluid force was measured by force transducers and the components in phase with cylinder velocity and acceleration were extracted as the Fourier averages over many cycles of oscillation. The experiments were conducted at the MIT Testing Tank facility using a mechanical device capable of translate the cylinder at constant velocity trough the tank and drive oscillations at the same time. Observe then that the turbulence of the incident flow is zero. Several test with different combinations of V^* and A^* were carried out. As it can be seen in Fig. 2, $C_Y \sin\phi$ may be positive for $5 < V^* < 9$ denoting energy transfer from the fluid to the cylinder. In addition, it is interesting to note the change in the sign of $C_Y \cos\phi$ at V^* around 6.

3.1.1. $m^* \gg 1$

In this case, at lock-in $f^* \simeq 1$ (see Eq. (3b)) and the key parameter to account for the mechanical properties is the combined mass-damping parameter $m^*\zeta$. Fig. 3 shows the efficiency behavior with the reduced velocity for three values of the mass-damping parameter. It is also shown the evolution of the normalized amplitude of oscillations. It can be seen that in all cases the maximum efficiency is reached almost at the same reduced velocity (around 5.8), as well as that the region of reduced velocities at which the efficiency is significant is narrower than that of the large scale oscillations. As $m^*\zeta$ decreases it seems that the region of significant efficiency increases. However, it seems that there is an optimum value of the mass-damping parameter for maximum efficiency. The relationship between the maximum efficiency attainable for a fixed value of the mass-damping parameter $m^*\zeta$ is shown in Fig. 4.

3.1.2. $m^* \sim 1$

For $m^* \sim 1$ the normalized frequency of oscillation strongly depends on the mass ratio. As was observed by Gharib [10] in his experiments, the frequency of oscillation increases monotonously with U^* without classical lock-in (see also [11]). The cylinder response (and therefore the efficiency) is then a function of the parameters m^*, ζ, U^*, as well as the Reynolds number (as previously said, this dependence is implicit in the fluid coefficients). To investigate this dependence we have performed numerical computations of A^*, f^* (Eqs. (3a) and (3b)), and efficiency (Eq. (6)) over a range of m^*, ζ, and U^*. Results are summarized in Figs. 5 and 6. The former explores the dependence of the efficiency with the mass ratio (Fig. 5a) and with the

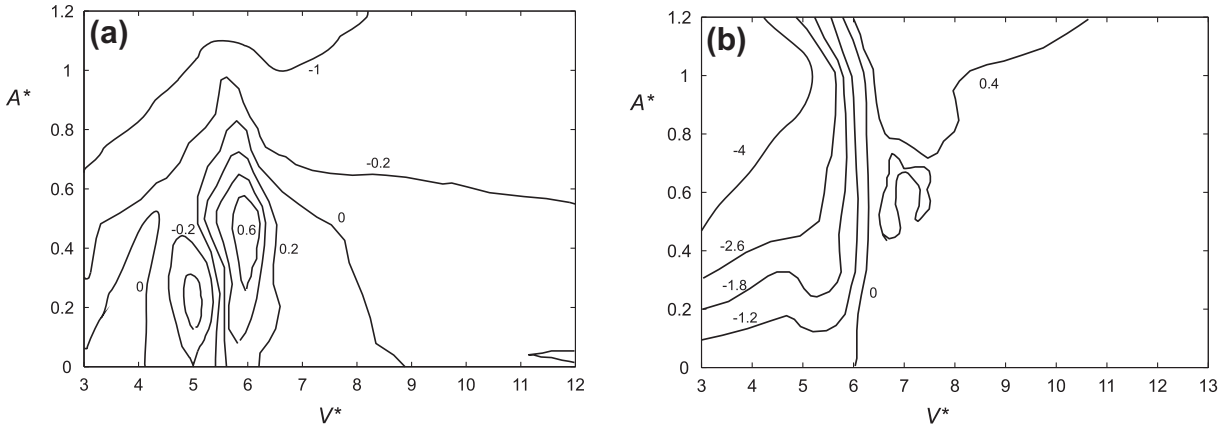

Fig. 2. Contour plot of $C_Y \sin\phi$ (a) and $C_Y \cos\phi$ (b) measured by Hover et al. [8].

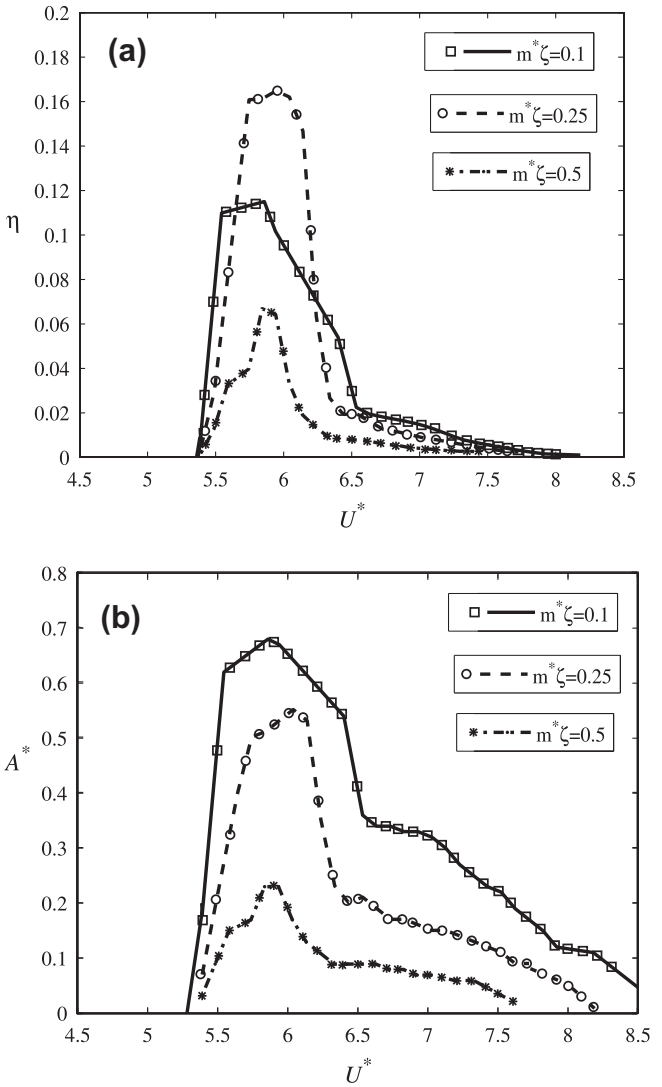

Fig. 3. (a) Energy efficiency for different values of the mass-damping parameter; (b) corresponding amplitudes of oscillations.

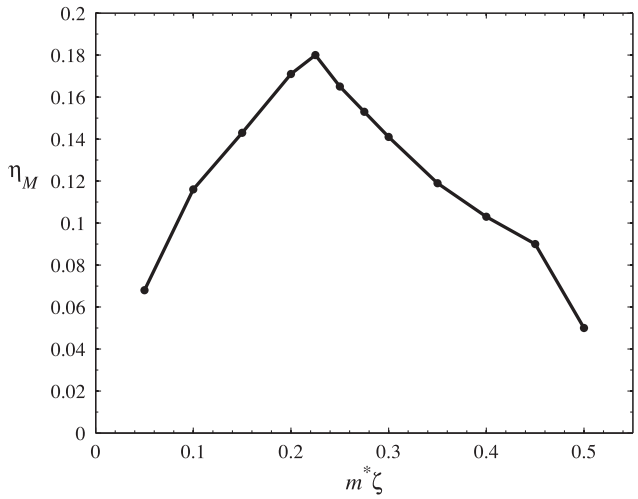

Fig. 4. Dependence of the maximum extraction of energy with the mass-damping parameter.

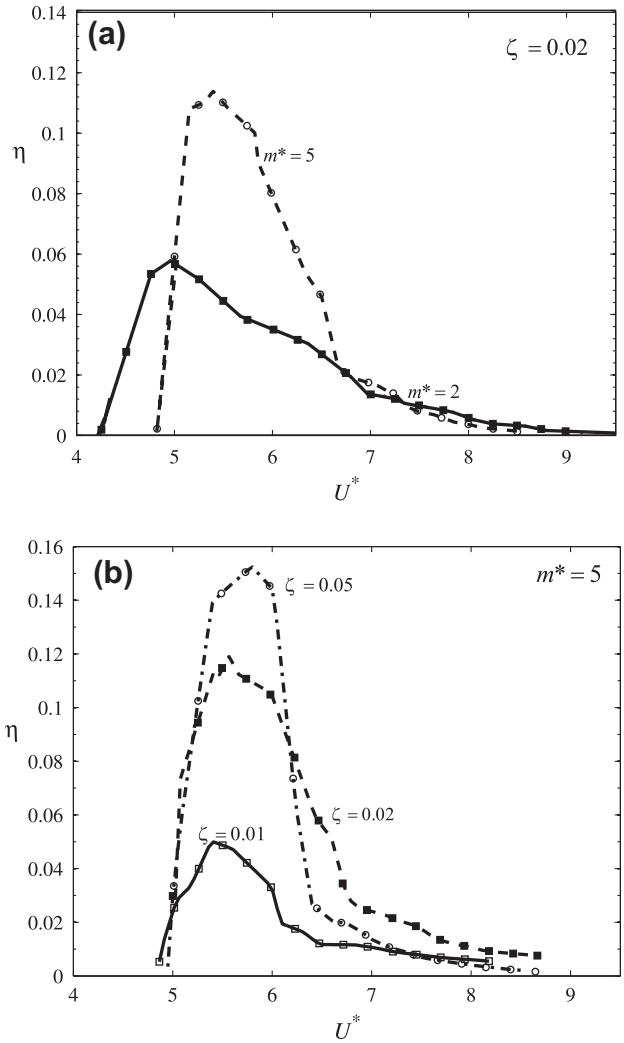

Fig. 5. Dependence of the energy efficiency with the mass-damping parameter (a) and the mechanical damping (b).

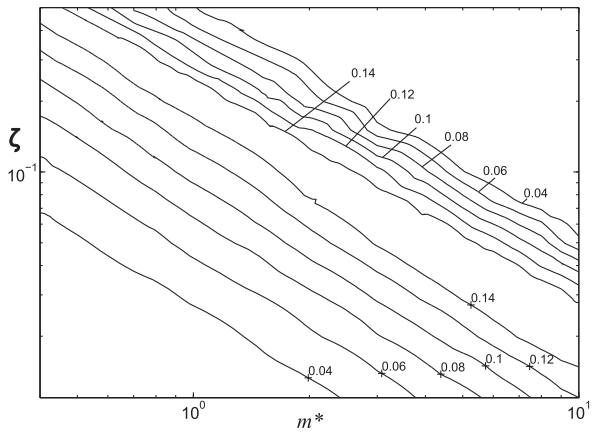

Fig. 6. Contour plot of the maximum efficiency η_M.

mechanical damping (Fig. 5b). From these plots one may see that the most notably effect of the mass ratio is on the range of reduced velocities where efficiency is significant, being increased for lower values. We believe that this is an expected behav-

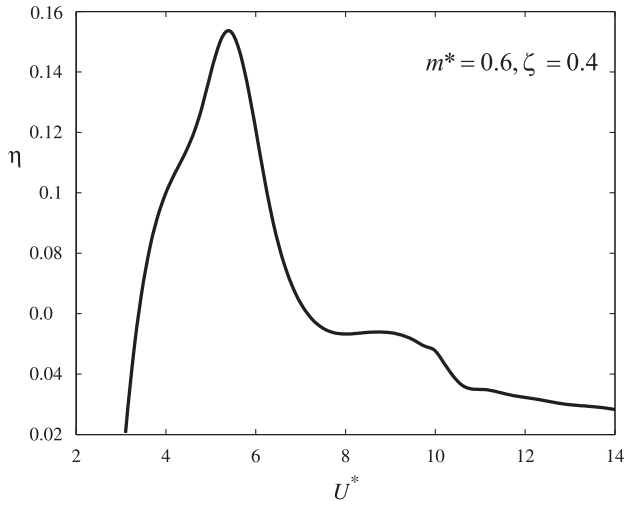

Fig. 7. High efficiency at a large range of flow velocities. $m^* = 0.6$ and $\zeta = 0.4$.

ior as it is a well established experimental fact that m^* controls the range of reduced velocity where oscillations are of significance. It is also seen (Fig. 5b) that the damping has a strong influence in the maximum efficiency attainable. In fact, the maximum attainable efficiency η_M might be again governed by the product $m^*\zeta$ (as in the case of $m^* \gg 1$). This point has been investigated in detail by computing η_M over a range of m^* and ζ. Results are presented in Fig. 6 in the form of a contour plot. It can be seen that isolines of maximum efficiency has a linear trend in a log–log plot, indicating a direct relationship between η_M and the mass-damping parameter $m^*\zeta$. We have also observed in from our computations the same for A_M^*. This last result is in agreement with Govardhan and Williamson [4] who argued that the peak amplitudes are controlled mainly by the product of $m^*\zeta$.

From a practical point of view, it is quite interesting to extract energy from a flow efficiently in a broad spectrum of environmental conditions (flow velocity). The above presented results suggest that it should be interesting to have a low mass ratio in order to enlarge the flow velocity range of significant efficiency and select the appropriate damping to get a high value of maximum efficiency; from Fig. 4 (also from Fig. 6) one may deduce that an optimum value is $m^*\zeta \sim 0.25$ (at the Reynolds regime under consideration). Fig. 7 shows the computed efficiency for mechanical parameters chosen from this criterium ($m^* = 0.6$; $\zeta = 0.4$). An efficiency higher that 0.1 is roughly obtained for $4 < U^* < 6.5$.

3.2. Influence of the Re regime

The efficiency dependence with m^* and ζ for a Reynolds number around 10^3 (Hover's experiments were carried out at a Reynolds number of 3800) has been presented in the previous sections. In the following we present the same study as

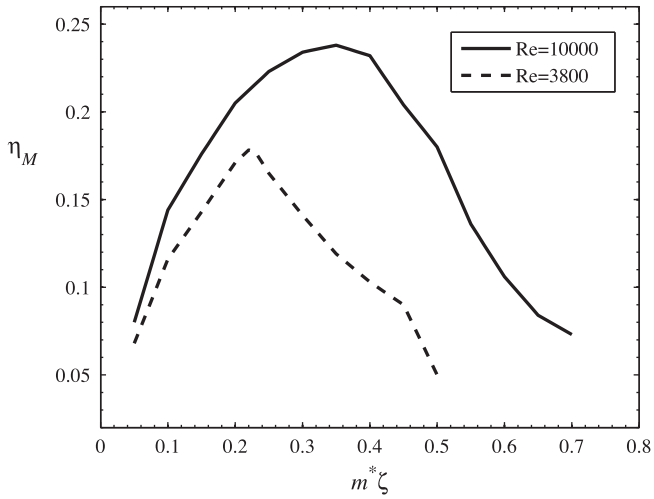

Fig. 8. Efficiency versus mass-damping parameter for two Reynolds numbers.

previously done but for a higher Reynolds number ($Re \sim 10^4$). The idea is to get a feeling about its influence in the energy conversion. To this end we have performed numerical computations in an identical way that in Section 3.1.1 using experimental data from Gopalkrishnan [9] who measured the fluid force coefficients of a circular cylinder with aspect ratio $L/D = 24$ forced to oscillate harmonically under the action of a cross-flow at a Reynolds number of 10,000.

The observed behavior from the computations was similar than that of the previous case ($Re \sim 10^3$), being the maximum efficiency mainly governed by the product $m^*\zeta$. The relationship between the maximum efficiency and the mass-damping parameter $m^*\zeta$ is shown in Fig. 8. It can be observed that efficiency is higher for the regime of large *Re* numbers. It seems also that the optimum value of $m^*\zeta$ is dependent on the *Re* number. Finally, we must note that computations show that the range of significant efficiency is also larger for the case of higher Reynolds number.

4. Conclusions

This study focuses on identifying the effect of governing parameters on the energy extraction efficiency by VIV. The main parameters investigated were the mass ratio, the mechanical damping coefficient, and the Reynolds number. Some key characteristics of performance can be outlined, like the maximum efficiency η_M attainable for fixed values of m^* and ζ or the range of flow velocities (reduced velocity) where efficiency is significant. The analysis carried out shows that: (i) η_M is mainly influenced by the mass-damping parameter $m^*\zeta$ and there is an optimum value of $m^*\zeta$ where η_M presents a maximum; (ii) the range of reduced velocities with significant efficiency is mainly governed by m^*; (iii) it seems that encouraging high efficiency values can be achieved for high Reynolds numbers. Finally, it must be noted, however, that the analysis herein presented should be seen only as an approximation to the real problem. For example, it is clear that the real VIV situation (a complete fluid–structure interaction problem) is more complex than that of a forced vibrations one, where the body is oscillating at a fixed amplitude and frequency. This point has been largely discussed in the literature, and the question of whether forced vibration tests can be used to predict VIV behavior has been addressed by several important investigators being still open. Nevertheless, recently, Morse and Williamson [12] have demonstrated that under carefully controlled conditions there is very close correspondence between free and forced vibration experiments. With this idea in mind, we believe that results presented in this paper can be representative and, from an engineering point of view, the parametric analysis of the present study can help to efficiently design a device to extract useful energy from VIV.

References

[1] C.H.K. Williamson, Vortex dynamics in the cylinder wake, Ann. Rev. Fluid Mech. 28 (1996) 477–539.
[2] P.W. Bearman, Vortex shedding from oscillating bluff bodies, Ann. Rev. Fluid Mech. 16 (1984) 195–222.
[3] T. Sarpkaya, A critical review of the intrinsic nature of vortex-induced vibrations, J. Fluids Struct. 19 (2004) 389–447.
[4] C.H.K. Williamson, R. Govardhan, Vortex-induced vibrations, Ann. Rev. Fluid Mech. 36 (2004) 413–455.
[5] M. Bernitsas, K. Raghawan, Y. Ben-Simon, E.M.H. Garcia, VIVACE (vortex induced vibration for aquatic clean energy): a new concept in generation of clean and renewable energy from fluid flow, J. Offshore Mech. Art. Eng., ASME Trans. 130 (2008) 041101.
[6] A. Barrero-Gil, G. Alonso, A. Sanz-Andres, Energy harvesting from transverse galloping, J. Sound Vib. 329 (14) (2010) 2873–2883.
[7] Q. Zhu, M. Haase, C.H. Wu, Modelling the capacity of a novel flow-energy harvester, Appl. Math. Model. 33 (2009) 2207–2217.
[8] F.S. Hover, A.H. Techet, M.S. Triantafyllou, Forces on oscillating uniform and tapered cylinders in cross-flow, J. Fluid Mech. 363 (1998) 97–114.
[9] R. Gopalkrishnan, Vortex Induced Forces on Oscillating Bluff Cylinders, Ph.D. Thesis, Massachusetts Institute of Technology, Cambridge, Massachusets, USA, 1992.
[10] M.R. Gharib, Vortex-Induced Vibration Absence of Lock-in and Fluid Force Deduction, Ph.D. Thesis, California Institute of Technology, Pasadena, USA, 1999.
[11] A. Khalak, C.H.K. Williamson, Dynamics of a hydroelastic cylinder with very low mass and damping, J. Fluids Struct. 10 (1996) 455–472.
[12] T.L. Morse, C.H.K. Williamson, Prediction of vortex-induced vibration response by employing controlled motion, J. Fluid Mech. 634 (2009) 5–39.